DOI 10.1007/s11595-016-1378-8

Corrosion Behavior of Ultra-high Strength Steel 300M in Different Simulated Marine Environments

GUO Qiang, LIU Jianhua*, YU Mei, LI Songmei

(Key Laboratory of Aerospace Materials and Performance (Ministry of Education), School of Materials Science and Engineering, Beihang University, Beijing 100191, China)

Abstract: Corrosion behavior of 300M in neutral corrosion environments containing NaCl simulated by total immersion (TI), salt spraying (SS) and periodic immersion (PI), was investigated by surface analysis techniques, corrosion weight-loss method, and electrochemical measurements. In total immersion environment, rust on the steel consisted of a porous outer rust layer with main constituent of γ-FeOOH, and an inner rust layer of dense Fe_3O_4 film with network broad cracks. In salt spraying environment, outer rust with main composition of γ-FeOOH/α-FeOOH/Fe_3O_4 was compact, and inner rust showed dense Fe_3O_4 film. Rust formed by periodic immersion exhibited a compact outer rust layer with constituent of α-FeOOH/γ-FeOOH/Fe_3O_4 and an inner rust layer with composition of α-FeOOH/α-Fe_2O_3; inner rust showed a ultra-dense film adherent to the steel. The corrosion rate showed a rule of v_{ss}(salt spraying)>v_{ti}(total immersion)>>v_{pi}(periodic immersion) in 0-240 h, and $v_{ss} \approx v_{ti} \gg v_{pi}$ in 240-720 h. The rust formed by periodic immersion was dense and compact, with stable electrochemical properties, and had excellent protection on the steel. Humidity and oxygen concentration in all the environments played major roles in rust formation.

Key words: ultra-high strength steel; corrosion; simulated corrosion environments; chloride

1 Introduction

In recent decades, corrosion problems for military equipments and civil transportation have been paid great attention. Corrosion problems cost the USA military about $20 billion per year, and the USA national cost for corrosion took about 3.1% of GDP[1]. A large proportion of aircraft crashes were caused by corrosion problems, particularly in aggressive atmospheric environments, such as coastal and marine atmospheric environments, which contained abundant air-borne salinity. Considering the service safety, aircraft structural materials have been paid extra attention to especially ultra-high strength steel, which is a kind of important structural material widely used in aviation industry and other fields.

300M is a kind of medium carbon low alloy ultra-high strength steel, with some addition of Mo and Si on the basis of AISI 4340[2-4]. Compared with AISI 4340, the mechanical and anti-SCC properties have been remarkably improved. So far, 300M has been a kind of the most successful UHSS, which is widely applied in landing gears of aircraft. Nowadays, 300M is also applied in other industries, such as weapon, petrochemical and automobile industries, *etc*[5,6].

It has been widely accepted that atmospheric corrosion of steels is affected by different environmental factors, such as humidity, wetting time, temperature and electrolyte thickness, *etc*. Total immersion test is a kind of simple and practical method usually used for evaluation of material reliability and weatherability. Salt spraying test is commonly used to simulate marine atmospheric corrosion environment. García[7] and Pérez[8-10] estimated the service life of weathering and carbon steels in simulated marine atmospheric environment by total immersion corrosion method, and found that porous rust on the steels in Cl-containing solution included γ-FeOOH, the most abundant, and α-FeOOH, Fe_3O_4, and adherent rust on CS and WS was Fe_3O_4, and γ-Fe_2O_3, respectively.

(Received: Feb. 13, 2015; Accepted: Apr. 21, 2015)

GUO Qiang(郭强): Ph D;E-mail: guoqiang832003@163.com

*Corresponding author: LIU Jianhua(刘建华): Prof.;E-mail liujh@buaa.edu.cn

Funded by the National Natural Science Foundation of China(No.51171011)

Sun[11,12] and Yu[13-15] investigated corrosion behavior of 300M and AF1410 in simulated marine atmospheric environment by salt spraying test, and found that the outer rust on the steels was mainly composed of γ-FeOOH. Above-mentioned work was all operated under the continuous condition. The atmospheric corrosion is widely accepted as an alternate wet-dry process. Periodic immersion corrosion test is usually used to simulate wet-dry alternate corrosion process. Wang[16] performed simulated marine atmospheric corrosion on steels with periodic immersion corrosion test, and found that rust showed fine particles and dense structure. Nishimura[17] demonstrated that ultra-fine iron oxide in rust formed during periodic immersion corrosion process, which increased rust impedance, and decreased the corrosion rate. It was shown that the continuous or discontinuous state remarkably affected the rust formation and corrosion process of steels.

In the present work, total immersion, salt spraying and periodic immersion corrosion methods, which simulated continuous or discontinuous corrosion environments, were performed in comparison to study the effect on corrosion behaviors of 300M in Cl-containing environment with different corrosion states, such as in solution, under thin solution film, and gradually thinning solution film. SEM was used to observe the surface morphology of rust on the steel; rust composition was analyzed by XRD and Raman spectroscopy. Corrosion behaviors were investigated by corrosion weight-loss and electrochemical measurements.

2 Experimental

2.1 Materials

The main chemical composition of 300M is shown in Table 1. The heat treatment system and microstructure of the steel were mentioned in previous work[18]. The specimen size for corrosion weight-loss tests was about 65 mm×35 mm×2.5 mm with exposed area of 1800 mm^2. And the exposed area of specimens for electrochemical measurements was about 78.5 mm^2. All specimens in the work were ground by emery paper up to grade 2000$^{\#}$, cleaned with acetone and anhydrous alcohol by ultrasonic sound, respectively.

Table 1 Main chemical composition of 300M steel/wt%

C	Ni	Cr	Si	Mn	Mo	V	Fe
0.40	1.90	0.71	1.66	0.64	0.37	0.088	Balance

2.2 Corrosion methods

The total immersion test referred to ASTM G31-04. The solution was 3.5wt% NaCl solution at 35±1 ℃ with pH≈6.9. The specimens were laid parallel to the horizontal level in the solution. The solution was refreshed in 7 d.

Neutral salt spraying test was conducted according to ASTM B117-97. The solution was 3.5wt% NaCl solution with pH≈6.9 at 35±1 ℃. The angle between specimens and horizontal level was about 30°.

Periodic immersion corrosion test referred to ASTM G44-99. Periodic immersion test took two stages: total immersion time for 10 min in 3.5wt% NaCl solution and exposure time of 50 min in the environmental chamber at 35±1 ℃ and relative humidity 45%±2% under exposure to far-infrared light. The solution was 3.5wt% NaCl solution with pH≈6.9 at 35±1 ℃, which was refreshed in 7 d.

Rust on the steel was removed by immersion in the mixture solution with 500 mL HCl/500 mL H_2O/3.5 g $C_6H_{12}N_4$ for 10 min. The specimen weight was determined before corrosion tests and after rust removal. The corrosion rate was calculated according to formula (1):

$$v = \frac{W_a - W_b}{S \times t} \times 1\,000 \tag{1}$$

where, v denotes the corrosion rate of the steel, mg·cm^{-2}·h^{-1}; W_b is the specimen weight before corrosion test, g; W_a is the specimen weight after rust removal, g; t is the corrosion time, h; S denotes the exposure area on the specimens for corrosion test, cm^2.

2.3 Characterization and measurements

Field emission scanning electron microscopy (FE-SEM, Apolloo300, CamScan, UK) was used to observe the surface morphology of inner and outer rust on the steel. Outer rust was ground into fine powders, and analyzed by XRD (D/max-2200, Rigaku, Japan) under operating conditions using Cu target with electric current 40 mA and electric voltage 40 kV at a scanning rate 6 °/min. Raman spectroscopy (Lab RAM HR800, Horiba JR, France) was employed to detect the inner rust. The electrochemical measurements were carried out on the rusted steel by electrochemical working station (VersaSTAT MC-4, Ametek, USA), in a traditional 3-cell electrochemical system with KCl saturated calomel electrode (SCE) as the reference electrode, a grand square platinum plate (20 mm× 20 mm) as the counter electrode and the rusted steel as the working electrode. Electrochemical impedance

spectroscopy (EIS) was operated in a frequency range from 100 kHz to 10 MHz and a sinusoidal voltage of 10 mV. Potentiodynamic polarization curves were performed from −250 mV (*vs* E_{oc}) to 0 mV (*vs* E_{ref}) with a sweep rate of 0.5 mV/s.

3 Results

3.1 Corrosion weight-loss test

Fig.1 shows the corrosion rate of the steel in different simulated corrosion environments with respect to corrosion time. In the three corrosion environments, corrosion rate decreases with increasing corrosion time. In 0-240 h, the corrosion rate of salt spraying (v_{ss}) is the most rapid in the three corrosion environments, and the corrosion rate of total immersion (v_{tl}) is lower than that of salt spraying (v_{ss}); the corrosion rate in periodic immersion environment is the slowest in all simulated environments. However, the corrosion rates of salt spraying and total immersion approach to each other in 240-720 h. In 240-720 h, the corrosion rates in all environments kept stable.

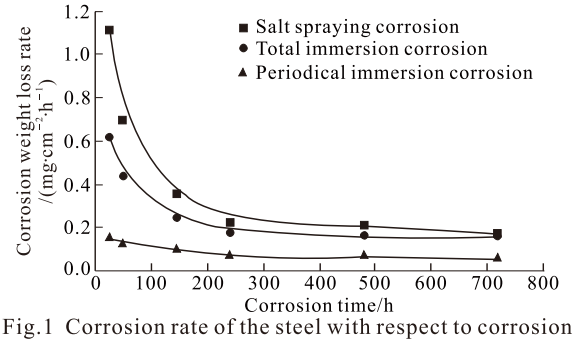

Fig.1 Corrosion rate of the steel with respect to corrosion time exposed in different corrosion environments

The three corrosion environments show features with similar NaCl concentrations, with the same temperature, different humilities and oxygen concentrations on the surface of the steel. It is indicated that humidity and oxygen concentration results in different corrosion rates. The stable corrosion rate in the corrosion environments in 240-720 h reflects that rust has remarkable effect on corrosion behavior after rust covered the whole surface of the steel.

3.2 Surface morphology

Fig.2 shows the macroscopical images of inner and outer rust on the steel formed in the three corrosion environments. Outer rust after total immersion corrosion is porous and loose, and inner rust is a dense film, as shown in Figs.2 (a, b). In salt spraying environment, outer rust on 300M was distributed in lath along the current flow, with good bonding with dense inner rust, as shown in Figs.2 (c, d). In Figs.2 (e, f), outer rust formed by periodic immersion corrosion is homogenous and compact, and inner rust is brown dense film, with excellent bonding with outer layer.

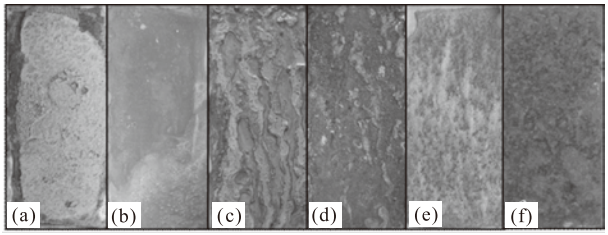

Fig.2 Macroscopical surface morphology of rust on the steel exposed in different simulated environment for 480 h Total immersion: (a) outer rust; (b) inner rust; salt spraying; (c) outer rust; (d) inner rust; periodic immersion; (e) outer rust; (f) inner rust

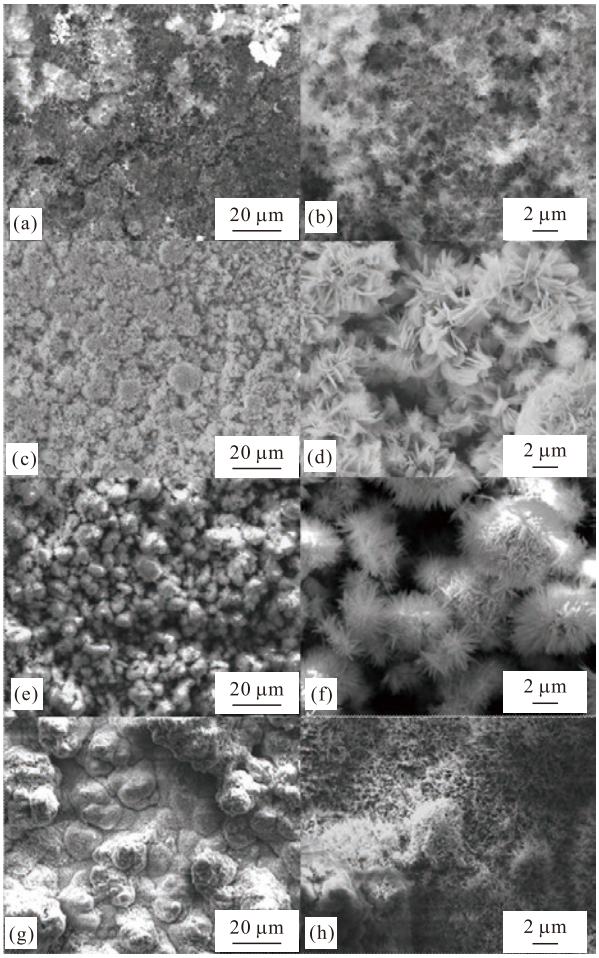

Fig.3 Surface morphology of outer rust on the steel exposed in different simulated environments for 240 h and 480 h (a, b: enlargation of a) Total immersion; (c, d, e, f: local enlargation of c, d) Salt spraying; (g, h local enlargation of g) Periodic immersion

Fig.3 shows the microscopical surface morphology of outer rust on 300M exposed in different corrosion environments. Figs.3(a-b) present the surface morphology of outer rust after total immersion corrosion. Outer rust after total immersion corrosion is

porous, and is mainly composed of ultra-fine acicular corrosion product, which represents γ-FeOOH[19,20]. Figs.3(c-f) show that outer rust formed by salt spraying is porous, and heterogeneous in microscopical morphology. Outer rust shows flakes and flocculus-like particles located in different regions, which are typical morphologies of α-FeOOH[19,20] and γ-FeOOH[20], respectively. Outer rust layer after periodic immersion corrosion exhibits compact and consists of acicular sphere particles.

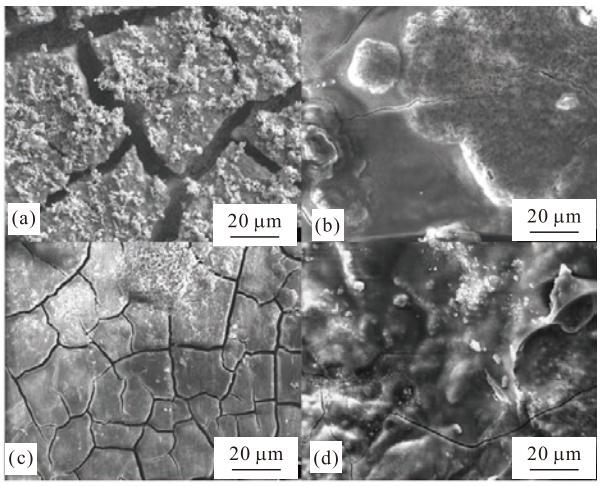

Fig.4 Surface morphology of inner rust on the steel exposed in different simulated environment for 480 h: (a) Total immersion; (b, c) Salt spraying; (d) Periodic immersion

Fig.4 shows inner rust on the steel formed in different environments. Compared with outer rust, inner rust shows a much denser film. Inner rust for total immersion is dense with network broad cracks. Most inner rust formed by salt spraying is dense without cracks, but some parts of inner rust contain network narrow cracks. The inner rust formed by periodic immersion is much denser with few narrow cracks.

3.3 Rust composition analysis

Fig.5 (a) shows the XRD results of outer rust on 300M exposed in different corrosion environments. According to the intensity of the composition in XRD, outer rust for total immersion is mainly composed of most abundant γ-FeOOH and the other Fe_3O_4. Outer rust for salt spraying contains mainly γ-FeOOH/α-FeOOH/Fe_3O_4. γ-FeOOH is the most abundant composition in the outer rust; the content of α-FeOOH is less than γ-FeOOH. The composition of outer rust contains α-FeOOH/γ-FeOOH/Fe_3O_4, in which α-FeOOH is the most abundant, with γ-FeOOH next to α-FeOOH.

Fig.5 (b) shows the Raman spectra of inner rust on 300M exposed in the different environments. In the Raman spectra, the characteristic peak at 680 cm^{-1} is assigned to Fe_3O_4. The characteristic peaks of γ-FeOOH are 255, 380, 528, 654, 1 054, and 1 307 cm^{-1}[21,22]. Peaks at 225 cm^{-1}, 295 cm^{-1} confirm existence of α-Fe_2O_3[21,22]. Characteristic peaks at 299 cm^{-1} and 397 cm^{-1} belong to α-FeOOH[21,22].The Raman reflection of γ-FeOOH mainly attributes to the residual of outer rust. Inner rust on 300M formed by total immersion and salt spraying is Fe_3O_4; and inner rust formed by periodic immersion is mainly composed of α-FeOOH/α-Fe_2O_3.

3.4 Electrochemical measurements

Figs.6 (a-c) show Nyquist plots of the rusted steels exposed for 240 h and 480 h in different environments. A well-defined loop is shown in Nyquist plots of rusted steel exposed for 240 h and 480 h, respectively. In the total immersion and salt spraying environments, compared with Nyquist plots at 240 h, the radius of the

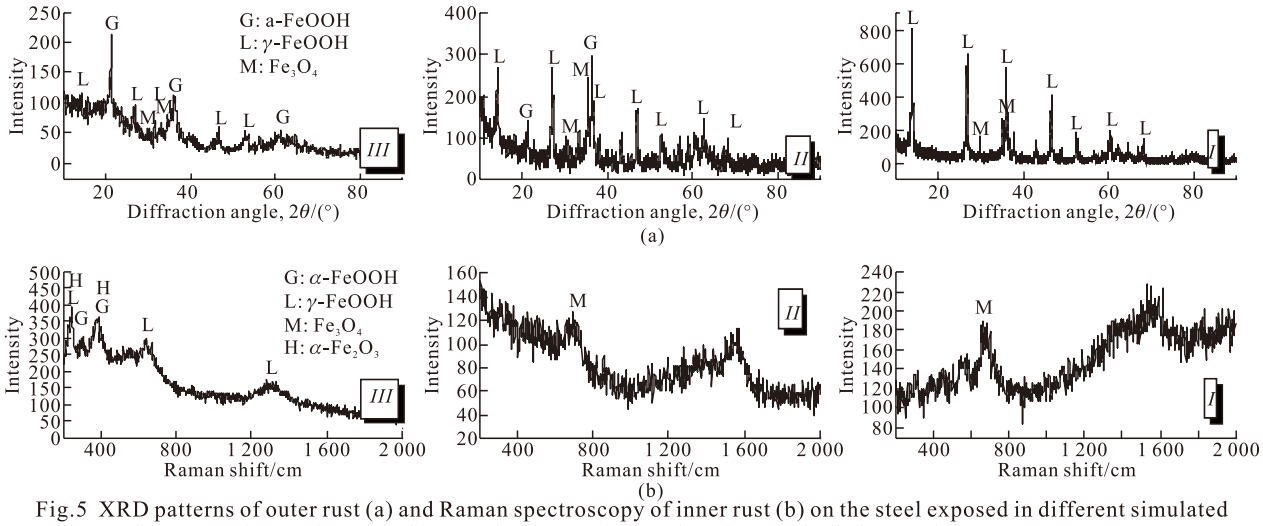

Fig.5 XRD patterns of outer rust (a) and Raman spectroscopy of inner rust (b) on the steel exposed in different simulated environments for 480 h (I) Total immersion; (II) Salt spraying; (III) Periodic immersion

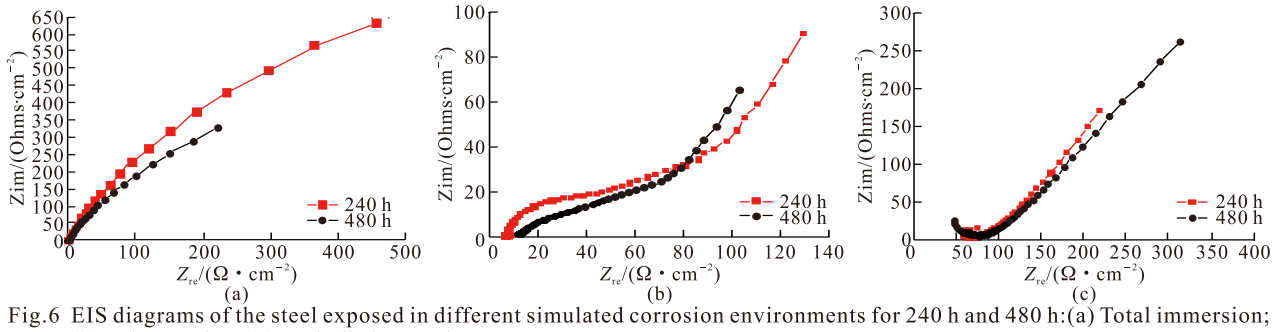

Fig.6 EIS diagrams of the steel exposed in different simulated corrosion environments for 240 h and 480 h:(a) Total immersion; (b) Salt spraying; (c) Periodic immersion

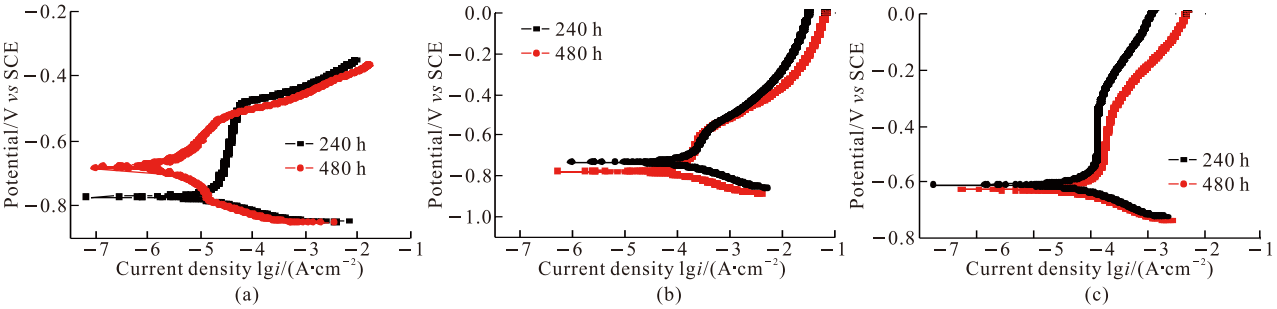

Fig.7 Potentiodynamic polarization curves of the steel exposed in different simulated corrosion environments for 240 h and 480 h: (a) Total immersion; (b) Salt spraying; (c) Periodic immersion

loop at 480 h decreased. It is indicated that corrosion resistance of rust decreased with corrosion time. The Nyquist plots of periodic immersion show two loops at low and high frequency, respectively; the radiuses of the loops at low frequency increased from 240 h to 480 h. It is indicated that in periodic immersion environment, the rust corrosion resistance increased with corrosion time.

Figs.7 (a-c) present potentiodynamic polarization curves of the rusted steels exposed for 240 h and 480h in different corrosion environments. In the salt spraying and periodic immersion, the same cathodic slope is shown at 240 h and 480 h, respectively. The cathodic slope for total immersion decreased from 240 h to 480 h. It is indicated that the rust effect on corrosion behavior increased from 240 h to 480 h in total immersion environment, but unchanged in salt spraying and periodic immersion environments.

For total immersion, the corrosion potential at 480 h decreased and corrosion current density increased according to that at 240 h. But the corrosion potential increased with corrosion time increasing from 240 h to 480 h in environments of salt spraying and periodic immersion, and corrosion current density decreased in periodic immersion environment, but increased for total immersion and salt spraying. It is indicated that rust on 300M for periodic immersion has excellent anti-corrosion properties and rust inhibited corrosion. However, rust for total immersion and salt spraying environments increased corrosion rate.

4 Discussion

4.1 Composition and formation of rust

The outer rust on the steel formed in total immersion environment was very porous and loose; the inner rust had broad cracks in network. The outer rust formed by salt spraying was compact, and had good bonding with inner rust. The inner rust was dense and homogenous, partly with narrow grid-like cracks. The outer rust on 300 M in total immersion environment was composed of γ-FeOOH/Fe_3O_4; inner layer was dense Fe_3O_4 film. The composition and morphology of outer rust on 300M formed by salt spraying were inhomogeneous, with main flocculus-like γ-FeOOH and flake α-FeOOH, also some Fe_3O_4; inner rust was dense Fe_3O_4 film. Outer rust formed by periodic immersion was composed of α-FeOOH/γ-FeOOH/Fe_3O_4, in which α-FeOOH was the main composition. The inner rust formed by periodic immersion was α-FeOOH/α-Fe_2O_3 dense film. There was good bonding force between inner and outer rust.

Corrosion process in total immersion and salt spraying environments was in continuous state. The morphology and composition of outer rust formed in the two environments were different, and inner rust

contained the same composition. The specimens of total immersion corrosion test were totally immersed in the solution. Oxygen was homogenously distributed on the steel. The morphology of outer rust had little difference. But solution film on the steel was different in thickness by effect of solution current in the salt spraying, and rust formed in lath along the solution current. Due to the difference in thickness of solution film and oxygen concentration, outer rust formed with different morphologies and compositions.

In the total immersion environment, rust formation process is shown as formula (2). Iron was dissolved into Fe^{2+}, and $Fe(OH)_2$, Fe(OCl). H_2O was transformed into γ-FeOOH. Subsequently, γ-FeOOH was reduced into Fe_3O_4. In the salt spraying environment, Cl^- ion facilitates the transformation of γ-FeOOH into α-FeOOH[23] as shown in formula (3). Periodic immersion corrosion process proceeded in discontinuous state. The electrochemical reactions in wet stage were the same with total immersion corrosion test. In the dry corrosion stage, corrosion would not occur in the environment with the humidity about 45%; γ-FeOOH agglomerated into particles, and γ-FeOOH transformed into α-FeOOH under surficial rust. The rust formed from the bottom to upside, and became a homogenous and dense layer gradually.

Anodic reaction: $Fe \rightarrow Fe^{2+}+2e$

Cathodic reaction: $O_2+2H_2O+4e \rightarrow 4OH^-$

Total reactions:

$$\begin{aligned} &Fe^{3+}+2Cl^-+OH^- \rightarrow FeOCl+HCl \\ &FeOCl \cdot H_2O \rightarrow \gamma\text{-}FeOOH \xrightarrow{e} Fe_3O_4 \\ &Fe(OH)_2 \rightarrow \gamma\text{-}FeOOH \end{aligned} \quad (2)$$

$$\begin{aligned} &\gamma\text{-}FeOOH \xrightarrow{\text{Chlorination}} FeO_x(OH)_{2-2x}Cl \\ &\xrightarrow{\text{Solidstate}} \alpha\text{-}FeOOH \end{aligned} \quad (3)$$

4.2 Rust effect on corrosion behavior

The corrosion weight-loss test indicates that in the initial period, the corrosion rate in salt spraying environment was the most rapid in the three environments; total immersion corrosion environment took the second place. Due to thin solution film on steel 300M in salt spraying environment, O_2 diffusion exhibited very fast; and rust was washed down by the descending solution current under the action of gravity, and corrosion area expanded faster than the others. As results, in the initial period the corrosion rate under salt spraying was the most rapid. Low corrosion rate in periodic immersion was due to dense and homogenous rust with excellent electrochemical stability. With rust covering the whole surface of the steel, the corrosion rate decreased gradually and became stable.

The results of electrochemical measurements indicate that the rust formed in total immersion environment had effect on corrosion process. Outer rust formed by total immersion was porous, with poor adherence with inner rust, which exhibited no diffusion barrier effect on corrosive ions. The composition of rust formed by salt spaying was not distributed homogenously. Outer rust layer consisted of γ-FeOOH/α-FeOOH/Fe_3O_4, in which γ-FeOOH was the most abundant, and inner rust was composed of Fe_3O_4. Fe_3O_4 film had excellent electron conductivity. The EIS and polarization curves of total immersion and salt spraying showed contradiction with corrosion weight loss test, mainly due to cathodic reduction of abundant γ-FeOOH in outer rust and poor resistance of Fe_3O_4 in inner rust during electrochemical measurement. In fact, with increasing corrosion time, the inner and outer rust increased in thickness, and the density of outer rust increased, which could inhibit the oxygen diffusion and decreased the corrosion rate. On the contrary, the inner and outer rust formed by periodic immersion was mainly composed of α-FeOOH, which had excellent electrochemical stability. Therefore, the EIS and polarization curves showed better corrosion resistance with increasing corrosion time, which agreed with corrosion weight loss test. Moreover, the dense structure increased the anti-corrosion properties.

5 Conclusions

a) In total immersion, salt spraying, and periodic immersion corrosion environments, the corrosion rate of 300M in salt spraying environment (v_{ss}) was the most rapid, and followed by total immersion test (v_{tl}) in 0-240 h. Corrosion rate v_{ss} and v_{tl} approached to each other in 240-720 h. In 0-720 h, the corrosion rate of periodic immersion v_{pi} was much lower than that of salt spraying and total immersion test.

b) In total immersion environment, outer rust was porous and composed of ultra-fine γ-FeOOH/Fe_3O_4 particles, and inner rust showed a dense Fe_3O_4 film with network broad cracks. In salt spraying corrosion environment, outer rust was compact with main composition of γ-FeOOH/α-FeOOH/Fe_3O_4, and inner rust was dense Fe_3O_4 film. Outer rust formed by periodic immersion corrosion was dense α-FeOOH/γ-FeOOH/Fe_3O_4 layer, and inner rust was α-FeOOH/

α-Fe_2O_3 dense film. In all the environments, humidity and oxygen concentration were main factors which affected rust formation.

c) The rust on the steel formed by total immersion and salt spraying showed poor corrosion resistance. By contrast, the rust formed by periodic immersion had remarkable retarding effect on corrosion behavior.

References

[1] Solis, William M. *Defense Management Opportunities to Reduce Corrosion Costs and Increase Readiness: GAO-03-753*[R]. USA, United States General Accounting Office, 2003

[2] Liu YG, Li MQ, Luo J. The Modeling of Dynamic Recrystallization in the Isothermal Compression of 300M Steel[J]. *Mater. Sci. Eng. A*, 2013, 574(1): 1-8

[3] Tomita Y, Okawa T. Effect of Microstructure on Mechanical Properties of Isothermally Bainite-transformed 300M Steel[J]. *Mater. Sci. Eng. A*, 1993, 172(1-2): 45-51

[4] Figueroa D, Robinson MJ. The Effects of Sacrificial Coatings on Hydrogen Embrittlement and Re-embrittlement of Ultra High Strength Steels[J]. *Corros. Sci.*, 2008, 50(4): 1 066-1 079

[5] Zhang SS, Li MQ, Liu YG, *et al.* The Growth Behavior of Austenite Grain in the Heating Process of 300M Steel[J]. *Mater. Sci. Eng. A*, 2011, 528(15): 4 967-4 972

[6] Luo J, Li MQ, Liu YG, *et al.* The Deformation Behavior in Isothermal Compression of 300M Ultrahigh-strength Steel[J]. *Mater. Sci. Eng. A*, 2012, 534: 314-322

[7] García KE, Morales AL, Barrero SA, *et al.* New Contributions to the Understanding of Rust Layer Formation in Steels Exposed to a Total Immersion Test[J]. *Corros. Sci.*, 2006, 48(9): 2 813-2 830

[8] Pérez FR, Barrero CA, Hight Walker AR, *et al.* Effects of Chloride Concentration, Immersion Time, and Steel Composition on the Spinel Phase Formation[J]. *Mater. Chem. Phys.*, 2009, 117(1): 214-223

[9] Pérez FR, Barrero CA, García KE. Factors Affecting the Amount of Corroded Iron Converted into Adherent Rust in Steels Submitted to Immersion Tests[J]. *Corro. Sci.*, 2010, 52(8): 2 582-2 591

[10] Pérez FR, Barrero CA, Arnache O, *et al.* Structural Properties of Iron Phases Formed on Low Alloy Steels Immersed in Sodium Chloride-rich Solutions[J]. *Physica B: Condensed Matter*, 2009, 404(8-11): 1 347-1 353

[11] Sun M, Xiao K, Dong CF, *et al.* Electrochemical Behaviors of Ultra High Strength Steels with Corrosion Products[J]. *Acta Metal Sin*, 2011, 47(4): 442(in Chinese)

[12] Sun M, Xiao K, Dong CF, *et al.* Electrochemical Corrosion Behavior of 300M Ultra High Strength Steel in Chloride Containing Environment[J]. *Acta. Metall. Sin. (Engl. Lett.)*, 2010, 23(4): 301-311

[13] Yu M, Qi JY, Liu JH, *et al.* Corrosion Behaviors of Ultra-high Strength Steel 40CrNi2Si2MoVA in Submerged Zone of Simulated Seawater[J]. *Corro. Pro*., 2011, 32(10): 778 (in Chinese)

[14] Hao XL, Liu JH, Li SM, *et al.* Effect of Neutral Salt Spray Precorrosion on Fatigue Life of AF1410 Steel[J]. *J. Aeronaut. Mater.*, 2010, 30(1): 67-71(in Chinese)

[15] Liu JH, Shang HB, Tao BW, *et al.* Corrosion Behavior of High Strength Steels 0Cr18Ni5 and AF1410[J]. *Mater. Eng.*, 2004, 8: 29-31(in Chinese)

[16] Wang ST, Yang SW, Gao KW, *et al.* Corrosion Behavior and Variation of Apparent Mechanical Property of a Novel Low Carbon Bainitic Steel in Environment Containing Chloride Ions[J]. *Acta Metall. Sin.*, 2008, 44(9): 1 116-1 124(in Chinese)

[17] Nishimura T, Katayama H, Noda K, *et al.* Effect of Co and Ni on the Corrosion Behavior of Low Alloy Steels in Wet/Dry Environments[J]. *Corros. Sci.*, 2000, 42(9): 1 611-1 621

[18] Liu JH, Tian S, Li SM, *et al*. Stress Corrosion Cracking of New Ultrahigh Strength Steel[J]. *Acta Aeronaut Astronaut Sin.*, 2011, 32(6): 1 164-1 170(in Chinese)

[19] Castaño JG, Botero CA, Restrepo AH, *et al.* Atmorpheric Corrosion of Carbon Steel in Colombia[J]. *Corros. Sci.*, 2010(52): 216-223

[20] Han SC. *Atlas of Microstructure on Metals Corrosion*[M]. Beijing: National Defense Industry Press, 2008: 11 (in Chinese)

[21] Dubois F, Mendibide C, Paginier T, *et al.* Raman Mapping of Corrosion Products Formed onto Spring Steels During Salt Spray Experiments. A Correlation between the Scale Compostion and the Corrosion Resistance[J]. *Corros. Sci.*, 2008, 50(12): 3 401-3 409

[22] Zhang X, Xiao K, Dong, CF, *et al.* In situ Raman Spectroscopy Study of Corrosion Products on the Surface of Carbon Steel in Solution Containing Cl^- and SO_4^{2-}[J]. *Eng. Fail. Anal.*, 2011,18: 1 981-1 989

[23] Ma YT, Li Y, Wang FH. Corrosion of Low Carbon Steel in Atmospheric Environments of Different Chloride Content[J]. *Corros. Sci.*, 2009, 51(5): 997-1 006